Analyst

Cite this: *Analyst*, 2012, **137**, 2827

www.rsc.org/analyst

PAPER

Two-channel microelectrochemical bipolar electrode sensor array†

Byoung-Yong Chang,[a] Kwok-Fan Chow,‡[b] John A. Crooks,§[b] François Mavré¶[b] and Richard M. Crooks*[b]

Received 22nd March 2012, Accepted 25th April 2012
DOI: 10.1039/c2an35382b

We report a two-channel microelectrochemical sensor that communicates between separate sensing and reporting microchannels *via* one or more bipolar electrodes (BPEs). Depending on the contents of each microchannel and the voltage applied across the BPE, faradaic reactions may be activated simultaneously in both channels. As presently configured, one end of the BPE is designated as the sensing pole and the other as the reporting pole. When the sensing pole is activated by a target, electrogenerated chemiluminescence (ECL) is emitted at the reporting pole. Compared to previously reported single-channel BPE sensors, the key advantage of the multichannel architecture reported here is physical separation of the ECL reporting cocktail and the solution containing the target. This prevents chemical interference between the two channels.

Introduction

Here we report a two-channel microelectrochemical sensor that communicates between separate sensing and reporting microchannels *via* one or more bipolar electrodes (BPEs).[1,2] Depending on the contents of each microchannel and the voltage applied across the BPE, faradaic reactions may be activated simultaneously in both channels. As presently configured, one end of the BPE is designated as the sensing pole and the other as the reporting pole. When the sensing pole is activated by a target, electrogenerated chemiluminescence (ECL) is emitted at the reporting pole. Compared to the single-channel BPE sensors we have reported previously,[3,4] the key advantage of the multichannel architecture is physical separation of the ECL reporting cocktail and the solution containing the target. This prevents interferences in both channels; that is, the ECL reaction is not quenched by the analyte,[5–7] and the ECL cocktail does not interfere with recognition of the target.

The first wireless electrochemical sensor was developed by Manz and co-workers using a U-shaped BPE.[8] The BPE sustained the reaction of $Ru(bpy)_3^{2+}$ or $Ru(phen)_3^{2+}$ with any one of three different target amino acids, which acted as co-reactants for the light-emitting process, and therefore the light intensity was directly related to the current through the BPE.[9,10] We expanded this concept to include protocols that do not require the analyte of interest to be directly coupled to the reporting reaction.[1] Using this approach, one pole of the BPE detects the target while the opposite pole reports the presence of the target *via* either ECL[4] or electrodissolution of Ag.[11] Because of charge conservation, the intensity of the reporting event is related to the recognition process at the sensing pole. Moreover, and as we have shown previously,[4,11,12] BPE-based sensors are inherently suitable for simultaneous operation of many electrodes using just a simple microchannel, a single power supply, and two driving electrodes. The two-channel approach reported here conserves these key advantages.

The method described here advances the functionality of a two-channel microelectrochemical ECL sensing device we previously reported.[13,14] That design was based on a standard electrochemical cell in which two microband electrodes were connected by a potentiostat, and the two channels were linked by a salt bridge. This configuration separates the sensing and reporting functions, but it does not incorporate the advantages of BPEs: specifically, simultaneous control of multiple electrodes and complete separation of the solutions in the reporting and sensing channels. We have reported a microelectrochemical system having two channels spanned by a BPE that concentrates charged analytes, but this device has no sensing function.[15] We have also previously described microelectrochemical devices, loosely related to the present system, that are able to carry out

[a]*Department of Chemistry, Pukyong National University, 45 Yongso-ro, Busan 608-739, Korea*
[b]*Department of Chemistry and Biochemistry, Center for Electrochemistry, Texas Materials Institute, and Center for Nano- and Molecular Science and Technology, The University of Texas at Austin 1 University Station, A5300 Austin, Texas 78712-0165, USA. E-mail: crooks@cm.utexas.edu; Tel: +1-512-475-8674*

† Electronic supplementary information (ESI) available: Experimental determination of the voltage between the anodic and cathodic poles of a BPE as a function of E_{tot}, and estimation of the minimum value of ΔE_{elec} required for ECL emission, are described in the ESI. See DOI: 10.1039/c2an35382b

‡ Current address: Kenan Laboratories of Chemistry, University of North Carolina, Chapel Hill, North Carolina 27599-3290, USA.

§ Current address: Department of Biochemistry, University of Wisconsin–Madison, 471 Biochemistry Addition, 433 Babcock Drive, Madison, WI, 53706, USA.

¶ Current address: Laboratoire d'Electrochimie Moléculaire, UMR 7591 CNRS, Université Paris Denis Diderot, Sorbonne Paris Cité, 15 rue Jean-Antoine de Baïf, F-75205 Paris Cedex 13, France.

logic operations using a complex arrangement of microchannels, traditional electrochemical cells, and BPEs.[16] Finally, Zhang and co-workers recently reported a closed BPE system that is also related to the device described here.[17]

Here, we demonstrate that sensing and reporting functions can be completely isolated from one-another, that arrays of multiple BPEs spanning separate channels can be controlled simultaneously, and that by varying the distance between the sensing and reporting poles different interfacial potential differences can be accessed within a single device. Finally, we show that a sensor based on this two-channel configuration is able to detect glycated hemoglobin (HbA_{1c}), which is the most important index for measuring the long-term average blood glucose level in the human body,[18,19] and report its presence by ECL.

Experimental

Chemicals

The following chemicals were purchased and used as received unless otherwise noted in the text: $Ru(bpy)_3Cl_2 \cdot 6H_2O$ (bpy = 2,2′-bipyridine), $K_3Fe(CN)_6$, tripropylamine (TPrA), thiophene-3-boronic acid (T3BA), and 4-ethylmorpholine from Sigma-Aldrich (Milwaukee, WI); NaCl and KCl from Fisher Chemical (Fairlawn, NJ); and glycated hemoglobin (HbA_{1c}) from Pointe Scientific, Inc. (Canton, MI). All aqueous solutions were prepared in doubly distilled water. The ECL solutions, which were comprised of $Ru(bpy)_3Cl_2$ and TPrA, were adjusted to pH 6.9 using 0.10 M phosphate buffer, and the solution containing $Fe(CN)_6^{3-}$ was prepared with 0.10 M KCl as the electrolyte. The HbA_{1c} solution contained 2.5 mM $K_3Fe(CN)_6$, 0.25 M KCl, and 0.10 M NaCl, and its pH was adjusted to 8.5 using 4-ethylmorpholine.[18]

Device fabrication

The interchannel BPEs were prepared on glass slides using standard lithographic methods we have described previously.[20] Briefly, a positive photoresist layer (~10 μm thick, AZ P4620) was deposited on Au-coated glass (5 nm Cr-adhesive layer and 100 nm Au layer, EMF Corp., Ithaca, NY) and exposed to UV light though a positive photomask containing the proper interchannel BPE design. After removal of the unexposed photoresist using developer solution (AZ 421 K, AZ Electronic Materials, Somerville, NJ), the unprotected Au and Cr layers were removed using, respectively, aqueous solutions containing 5% I_2 and 10% KI (for 2 min) and 9% $(NH_4)_2Ce(NO_3)_6$ 6% $HClO_4$ (for 30 s). Finally, the masked photoresist layer was removed in acetone. Immediately prior to use, the electrodes were cleaned in piranha solution (**Warning**: piranha solution is a strong oxidant, consisting of 30% H_2O_2 and 70% H_2SO_4 (v/v), that reacts violently with organic materials. It should be handled with extreme care, and all work should be performed under a fume hood and with protective gear). The Au microbands in each channel were 50 μm in width.

The microfluidic channels were prepared by soft lithography using poly(dimethylsiloxane) (PDMS) (Sylgard 184, Dow Corning, Midland, MI).[20,21] The dimensions of the channels were 1.0 cm long, 1.75 mm wide, and 28 μm high. Two 1.0 mm diameter reservoirs were punched at the ends of the channel to admit solutions and to accommodate the driving electrodes.

The glass base of the device, supporting the Au electrodes, and the PDMS monolith, containing the channel pattern, were treated with an air plasma for 15 s, pressed together, and then heated at 70 °C for 2 min.

Electrochemistry

Voltammetric measurements were made using a CHI 760B potentiostat (Austin, TX) and a standard three-electrode configuration; the working, counter, and reference electrodes consisted of a 2.0 mm diameter Au disk, a Pt mesh, and a Ag|AgCl (3.4 M KCl) electrode, respectively. All voltammograms were obtained under quiescent conditions. However, experiments involving bipolar electrodes were carried out by manipulating electric fields inside microchannels using a power supply, Lambda LLS9120. Voltages were applied to the microchannel *via* Au wire driving electrodes inserted into large reservoirs at either end of the channel.

Data acquisition

A microscope (Nikon AZ100, Nikon Co., Tokyo, Japan) equipped with a mercury lamp (Nikon), and a CCD camera (Cascade, Photometrics Ltd., Tucson, AZ) were used to obtain optical and ECL micrographs. Micrographs were initiated 4 s after application of the driving voltage, and the exposure time was 1.000 s. The resulting micrographs were analyzed by V++ Precision Digital Imaging software (Digital Optics, Auckland, New Zealand), which converts the brightness of each pixel on the 2D micrograph to photon counts. The ECL intensity was calculated by integrating the photon count for each pixel of the ECL-active area of the micrographs.

Results and discussion

Basic principles

Scheme 1a is a top view of the experimental configuration used to control a single BPE within a single microchannel. We have described this type of device in detail previously.[1,22] Briefly, however, a conductive material, which has no external electrical connection, is located inside a microchannel whose dimensions are small enough to ensure a high resistance to ionic current flow. A simple power supply applies a voltage difference, E_{tot}, between two driving electrodes situated in reservoirs at either end of the channel. Because the channel resistance is high, most of E_{tot} is dropped linearly along the channel length. Therefore, the interfacial potential difference between the solution and the poles of the BPE (ΔE_{elec}) may be sufficient to drive faradaic reactions. The magnitude of ΔE_{elec} (eqn (1)) depends on the length of the BPE (l_{elec}) and the magnitude of the electric field, which can be approximated as E_{tot} divided by the length of the channel ($l_{channel}$).

$$\Delta E_{elec} = \frac{E_{tot}}{l_{channel}} l_{elec} \quad (1)$$

For a pair of redox processes to occur simultaneously at the poles of the BPE, the value of ΔE_{elec} must, at a minimum, exceed the difference in the formal potentials of the two half reactions.

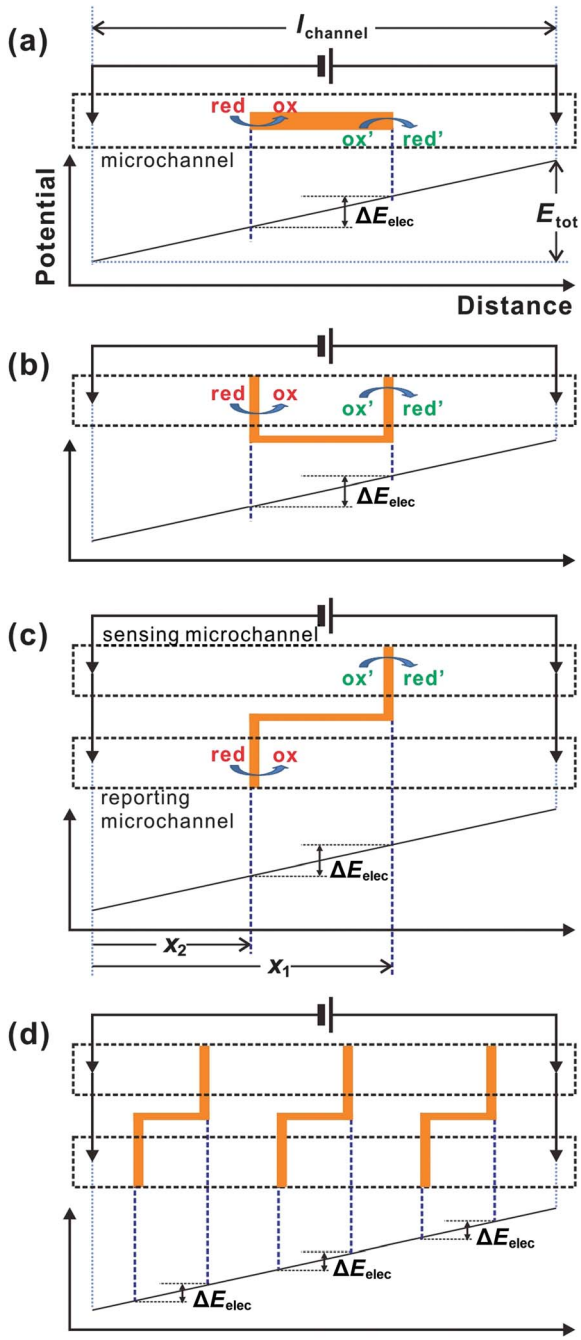

Scheme 1

Moreover, the cathodic and anodic electrochemical processes are coupled electrically *via* the BPE, and therefore they must occur at the same rate to ensure that electroneutrality is maintained within the conductive BPE. One final point: the potential of the BPE (E_{elec}) floats to a value that is in equilibrium with the surrounding solution.[1]

Scheme 1b illustrates the situation when a split BPE is present within a single channel.[15,22] In this case, the same value of E_{tot} is applied across the channels, and the relative separation of the poles of the split BPE is equivalent to l_{elec}. Accordingly, the interfacial potential between the solution and the BPE poles (ΔE_{elec}) is still given by eqn (1).

Scheme 1c illustrates the operating principle that governs a device having separate sensing and reporting electrodes situated in separate microchannels. Here, the sensing chemistry is carried out on the microband electrode in the top microchannel (sensing microchannel) and ECL reporting occurs near the microband electrode in the bottom microchannel (reporting microchannel). The advantage of this approach is that the two poles of the BPE can be exposed to different solutions, and hence the sensing and reporting functions are chemically decoupled. Accordingly, this design is ideally suited for sensing applications. Moreover, multiple BPEs may be used to span the two channels. If the spacing between the poles is the same for every BPE, as shown in Scheme 1d, then ΔE_{elec} is uniform. If the spacing differs, then different values of ΔE_{elec} will be experienced by each electrode. In both cases the value of E_{elec} is different for each BPE, but this does not affect device performance as only ΔE_{elec} matters from an electrochemical point of view.[23]

When two microbands located at positions x_1 and x_2 (Schemes 1b and c) are connected externally, the potential difference between the two microbands can be estimated using eqn (2).[22] This is true regardless of whether one or two channels house the two poles of the BPE.

$$\Delta E_{elec} = V_0(x_1 - x_2) \quad (2)$$

The potential profiles of the two channels in Schemes 1c and d should be the same, because the same driving voltages are applied to each. Hence the electric fields (V_0) in the microchannels may be expressed by eqn (3).

$$V_0 = E_{tot}/l_{channel} \quad (3)$$

However, eqn (3) implies that no potential is lost to faradaic reactions at the driving electrodes. This is, of course, not true, and therefore, in a real system, the potential profiles in the two channels may be slightly different if the solutions in the two channels are different.[22] Accordingly, in the experiments described later, we are careful to take into account the measured potential profiles rather than rely solely on a calculated estimate. The details of how these measurements were made are provided in the ESI (Fig. S1 and S2†).

When the two poles of a microband electrode are configured in separate microchannels and then connected externally (Schemes 1c and d), the measured equilibrium potential of the BPE lies between the solution potentials at positions x_1 and x_2. This means that the reduction reaction occurs where the potential of the BPE is lower than the solution potential, while the oxidation reaction occurs where the BPE potential exceeds the solution potential. The experiments reported here are configured so that the sensing reaction (reduction) occurs at x_1 in the sensing microchannel and the ECL reporting reaction (oxidation) occurs at x_2 in the reporting microchannel.

Interchannel BPE sensing and reporting

In the two-channel configuration, the sensing chemistry occurs in the sensing microchannel at the cathodic pole of the BPE. The state of the sensing reaction is accurately transmitted to the anodic pole of the BPE where it is reported as ECL luminescence

in a separate reporting channel. The sensing and reporting faradaic reactions will occur at the same time when ΔE_{elec} is larger than the onset potential (the minimum operating potential) of the two faradaic reactions.

The principle of interchannel BPE operation is demonstrated by filling the sensing channel with a conventional electroactive species, $Fe(CN)_6^{3-}$,[24] while the reporting channel is filled with an ECL cocktail. As discussed in the ESI (Fig. S3†), the difference in the onset potentials for the reduction of $Fe(CN)_6^{3-}$ and the oxidation of the ECL cocktail is 0.67 V. Therefore, when E_{tot} = 16.0 V, which corresponds to ΔE_{elec} = 0.69 V (Fig. S2†), ECL is observed at the anodic pole of the BPE. However, when E_{tot} < 16.0 V (*i.e.*, ΔE_{elec} < 0.69 V), ECL is not observed in the reporting microchannel.

Having demonstrated that ECL reporting can be tied to a sensing reaction through an interchannel BPE, we sought to demonstrate that this method is quantitative. Fig. 1a shows a two channel device spanned by a split BPE. The dashed white lines outline the two microchannels, and the burnt orange line emphasizes the location of the BPE. Solutions of $Fe(CN)_6^{3-}$, ranging in concentration from 0.10 to 5.0 mM, were then loaded into the sensing channel for each experiment, and the ECL cocktail was added to the reporting channel. The experiments described next were carried out under static (no intentional pressure driven flow) conditions.

The micrographs in Fig. 1b and c correspond to ECL emission at the anodic pole of the BPE when the concentrations of $Fe(CN)_6^{3-}$ are 0.10 and 5.00 mM, respectively. As suggested by these data, and shown explicitly in Fig. 1d, the ECL intensity is a linear function of the $Fe(CN)_6^{3-}$ concentration with a detection limit of 0.32 mM. Importantly, this sensing/reporting strategy can easily include any electroactive target; for example, the electroactive product of an enzymatic reaction, as long as it is reduced at a lower potential than that required for ECL emission.

The linear correspondence between ECL intensity and the concentration of $Fe(CN)_6^{3-}$ shown in Fig. 1d can be understood in terms of the electrochemical properties of the sensing and reporting reactions. These data (Fig. 2) were obtained using a conventional three-electrode cell. For the target molecule, $Fe(CN)_6^{3-}$, the *i–V* curve fits the theoretical expectation for an uncomplicated sampled-current voltammogram (SCV).[25,26] Accordingly, the cathodic current corresponding to the reduction of $Fe(CN)_6^{3-}$ is directly correlated to its concentration. The shape of the SCV obtained using the ECL reporting cocktail is similar to that of the target, but the current density is substantially higher due to the higher concentrations of $Ru(bpy)_3^{2+}$ and TPrA. Because electroneutrality must be maintained when the two half cells are linked by the BPE, the reduction of $Fe(CN)_6^{3-}$ limits the maximum current at both poles.[11,22] Therefore, the ECL intensity depends only on the rate of $Fe(CN)_6^{3-}$ reduction and hence its concentration in the sensing microchannel.

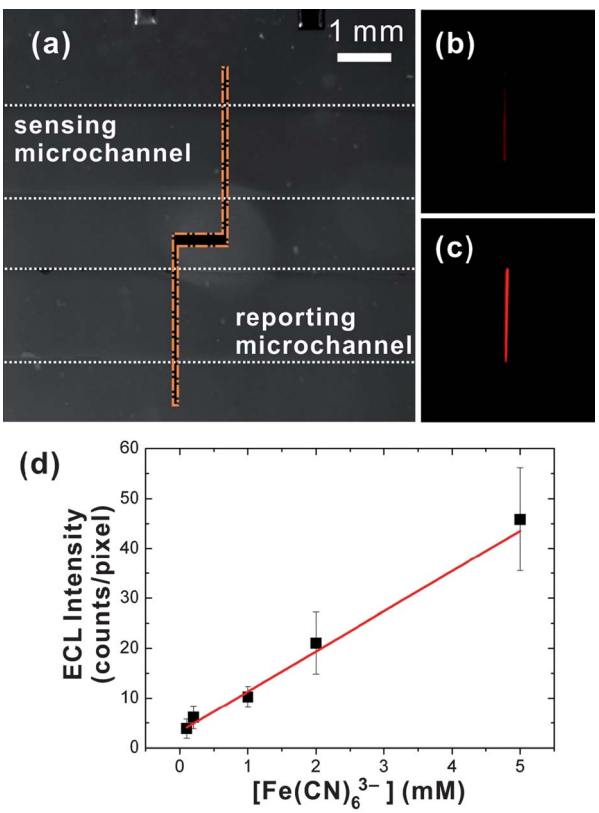

Fig. 1 (a) Micrograph of an interchannel BPE spanning parallel sensing and reporting microchannels. The individual poles of the BPE are 50.0 μm wide. The sensing microchannel was filled with the target molecule ($Fe(CN)_6^{3-}$) and the reporting microchannel was filled with the ECL cocktail (1.0 mM $Ru(bpy)_3^{2+}$ and 25 mM TPrA). Luminescence micrographs obtained with (b) 0.10 mM and (c) 5.0 mM $Fe(CN)_6^{3-}$ present in the reporting channel. (d) Plot of ECL luminescence intensity *vs.* the concentration of $Fe(CN)_6^{3-}$. E_{tot} = 16.0 V.

Interchannel BPE arrays

Scheme 1d illustrates a design that can be used to demonstrate the function of a small dual-channel, split BPE sensor array. Fig. 3 is an optical micrograph of such an array that consists of four BPEs, each having the same spacing (l_{elec} = 1.00 mm)

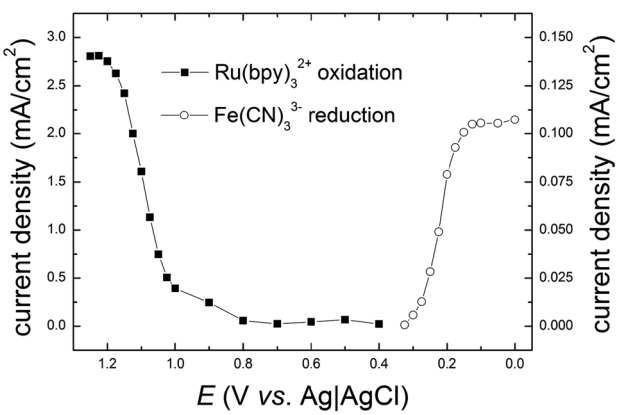

Fig. 2 Sampled-current voltammograms for the reduction of 5.0 mM $Fe(CN)_6^{3-}$ in 0.10 M KCl and for the oxidation of 1.0 mM $Ru(bpy)_3^{2+}$ and 25 mM TPrA in 0.10 M phosphate buffer solution. The $Fe(CN)_6^{3-}$ solution was degassed to remove oxygen. The data were obtained in a cell configured with a 2.0 mm diameter Au working electrode, a Pt counter electrode, and a Ag|AgCl reference electrode. The current was sampled 20 s after applying a desired potential step relative to the open circuit potential. The solutions were not stirred.

between the anodic and cathodic poles. As discussed in the Introduction, just a single pair of driving electrodes and one power supply is required to control all four BPEs. When a voltage of $E_{tot} = 20.0$ V is applied to the driving electrodes, the approximate value of ΔE_{elec} is 1.0 V (eqn (2)). Fig. 2 shows that this is more than sufficient driving force to reduce $Fe(CN)_6^{3-}$ and oxidize the ECL cocktail. Fig. 3b shows that under these conditions a robust ECL signal is observed from the anodic pole of each BPE, and Fig. 3c shows that luminescence intensity is reasonably uniform: the relative standard deviation of the maxima in the line scans is 5.0%.

Fig. 4a is an optical micrograph of a second type of BPE array. Here, the distances between the anodic and cathodic poles of each BPE are different due to the variable length of the interconnection between the microchannels. Specifically, the three electrodes, labeled i, ii, and iii, have $l_{elec} = 1.50$, 1.25, and 1.00 mm, respectively. This means that for a particular value of E_{tot}, ΔE_{elec} will be different for each BPE. Therefore, when a low driving voltage ($E_{tot} = 11.0$ V) is applied across the microchannels, only BPE i has a sufficiently high ΔE_{elec} to produce an ECL signal. However, an intermediate value of $E_{tot} = 13.0$ V is sufficient to drive ECL at BPEs i and ii (Fig. 4c). Finally, when E_{tot} is increased to 16.0 V, all three interchannel BPEs are illuminated (Fig. 4d). In this case, the ΔE_{elec} values for electrodes i, ii, and iii are 1.00, 0.86, and 0.69 V, respectively. Recall that $\Delta E_{elec} > 0.67$ V will drive both the sensing and reporting faradaic reactions (Fig. S3†).

Interestingly, when E_{tot} exceeds 19.0 V, ECL emission from electrode i turns off (Fig. 4e). Under these conditions, ΔE_{elec} for electrode i is expected to be 1.4 V. We believe that this high overpotential initiates background reactions, such as the oxidation of water, and this in turn leads to formation of oxygen that both chemically and physically (bubble formation on the BPE) interferes with ECL emission.[27] Even higher values of E_{tot} extinguish ECL luminescence at electrode ii (Fig. 4f) and eventually at all three BPEs. The important point, however, is that the microelectrochemical design shown in Fig. 4a is able to sense a range of potentials, and it is therefore suitable for driving

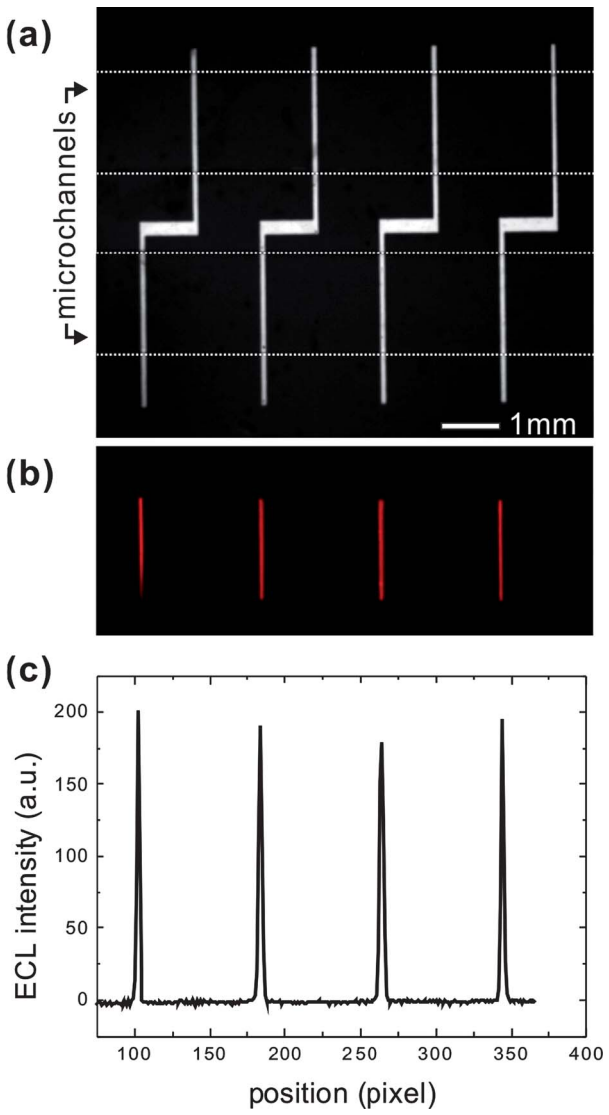

Fig. 3 (a) Optical micrograph of an array of four identical interchannel BPEs. The upper microchannel is the sensing microchannel and the lower microchannel is the reporting channel. The distance between the poles of each BPE is $l_{elec} = 1.00$ mm. (b) A luminescence micrograph of the BPEs in the reporting microchannel obtained at $E_{tot} = 20.0$ V. (c) A line scan obtained from (b) showing the ECL intensity of each electrode.

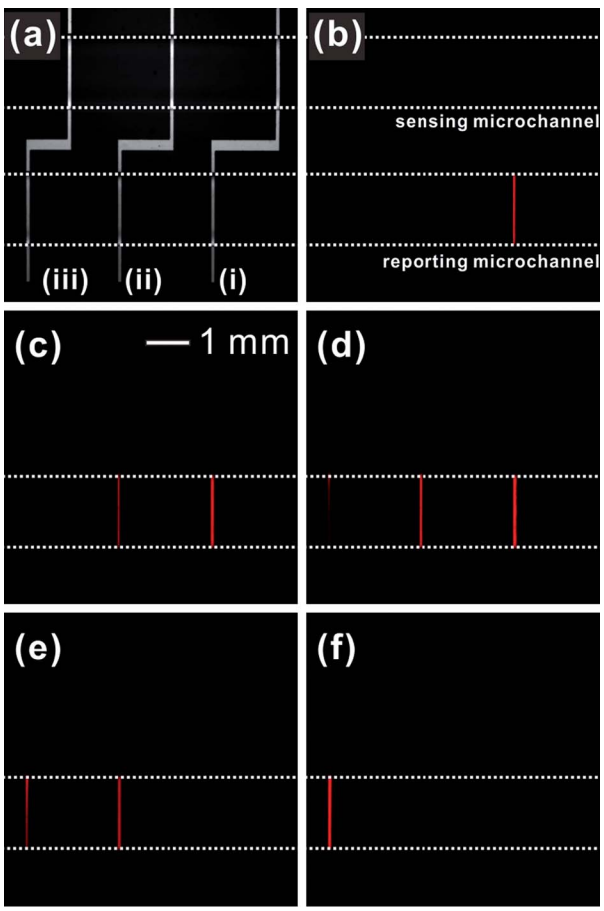

Fig. 4 (a) An optical micrograph of three interchannel Au BPEs having the following lengths (l_{elec}): i, 1.50 mm; ii, 1.25 mm; and iii, 1.00 mm. (b–f) Luminescence micrographs obtained with $E_{tot} = 11.0$, 13.0, 16.0, 19.0, and 22.0 V, respectively.

electrochemical reactions at different rates and for selecting individual electrodes to carry out specific electrochemical tasks in a single device.

Biosensing using interchannel BPEs

To demonstrate the potential capabilities of interchannel BPEs, HbA_{1c}, which is an important marker for blood glucose levels, was detected *via* ECL reporting. An array was fabricated consisting of two identical interchannel BPEs (Fig. 5a and b). The configuration of the device is the same as that described for Fig. 3, except just two BPEs are present. The sensing pole of the left-most electrode surface was modified with a drop of 10.0 mM T3BA in MeOH, which acts as a probe for HbA_{1c}.[16] The sensing pole of the other electrode was left naked (Fig. 5a). Next, a PDMS microchannel block was placed over the array, the sensing channel was filled with a standard solution containing 11 mg dL^{-1} HbA_{1c} as received from Pointe Scientific, Inc., and after 10 min this solution was removed, the channel rinsed, and then refilled with 5.0 mM $Fe(CN)_6^{3-}$. The reporting channel was filled with 1.0 mM $Ru(bpy)_3^{2+}$ and 25 mM TPrA. Finally, E_{tot} = 16.0 V was applied to both channels.

It has previously been shown that the binding of HbA_{1c} to T3BA at an electrode surface increases its impedance.[18,28]

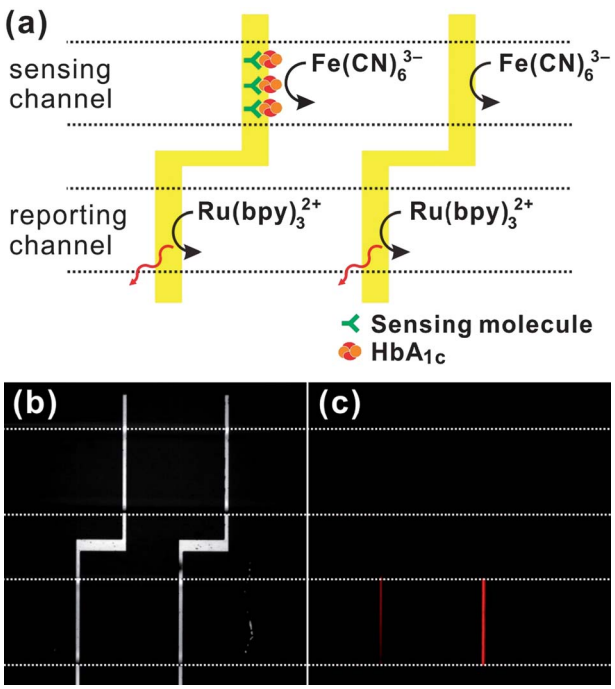

Fig. 5 (a) Scheme illustrating a proof-of-concept sensing experiment involving two interchannel BPEs. The left sensing pole is modified with a T3BA capture probe and the right sensing pole is unmodified. Detection of HbA_{1c} is observed as a reduced ECL emission on the reporting pole of the electrode on the left. (b) An optical micrograph of the array. The distance between the poles of the electrodes is l_{elec} = 1.00 mm. (c) An ECL micrograph of the array after exposure of the sensing poles to HbA_{1c}. The micrograph was obtained after removing the target from the sensing channel, and refilling it with the 5.0 mM $Fe(CN)_6^{3-}$. The reporting channel contained 1.0 mM $Ru(bpy)_3^{2+}$ and 25 mM TPrA. The solutions in the channels were static and E_{tot} = 16 V.

Accordingly, we expect the ECL emission from the T3BA-modified BPE to be reduced compared to its naked neighbor in the presence of HbA_{1c}. This expectation is borne out in Fig. 5c. Here, the ECL signal emitted from the bare Au electrode (on the right) is 71% brighter than the electrode modified with the probe. Clearly, this is a very simple demonstration of interchannel sensing, but it demonstrates the basic principle that a pair of BPEs can differentiate the presence of a target without interference from the ECL reporting chemistry.

Summary and conclusions

The main point of this paper is to show that sensing and reporting chemistry can be confined to individual microchannels spanned by BPEs. This results in separation of the chemistries in the two channels, which could interfere with one-another, while maintaining an electrochemical link. Because the latter results in equal currents at both the anodic and cathodic poles of the BPE, there is a direct link between sensing and ECL reporting. Another important result is that multiple BPEs can be used to span the two channels, and that the response of each BPE is about the same. This means that the device can be used in an array format. Moreover, even though only a single power supply and a single pair of driving electrodes is required to operate the device, each BPE can sense a different electrode/solution potential difference simply by varying the distance between the poles.

At present, we are studying two applications of this type of device. The first involves screening of electrocatalysts using an approach reported previously.[29] In addition, we are just beginning to carry out quantitative sensing experiments using medium-scale arrays of BPEs that span a single pair of channels. The results of these experiments will be reported in due course.

Acknowledgements

We gratefully acknowledge financial support from the U. S. Army Research Office (grant no. W911NF-07-1-0330) and the U. S. Defense Threat Reduction Agency. We also thank the Robert A. Welch Foundation (grant F-0032) for sustained support of our research activities. Byoung-Yong Chang was partially supported by a National Research Fund Grant funded by the Korean Government (NRF-2011-0009714).

References and notes

1 F. Mavré, R. K. Anand, D. R. Laws, K.-F. Chow, B.-Y. Chang, J. A. Crooks and R. M. Crooks, *Anal. Chem.*, 2010, **82**, 8766–8774.
2 G. Loget and A. Kuhn, *Anal. Bioanal. Chem.*, 2011, **400**, 1691–1704.
3 W. Zhan, J. Alvarez and R. M. Crooks, *J. Am. Chem. Soc.*, 2002, **124**, 13265–13270.
4 K.-F. Chow, F. Mavré and R. M. Crooks, *J. Am. Chem. Soc.*, 2008, **130**, 7544–7545.
5 J. McCall, C. Alexander and M. M. Richter, *Anal. Chem.*, 1999, **71**, 2523–2527.
6 W. Miao, *Chem. Rev.*, 2008, **108**, 2506–2553.
7 W. Cao, J. P. Ferrance, J. Demas and J. P. Landers, *J. Am. Chem. Soc.*, 2006, **128**, 7572–7578.
8 A. Arora, J. C. T. Eijkel, W. E. Morf and A. Manz, *Anal. Chem.*, 2001, **73**, 3282–3288.
9 F. Kanoufi and A. J. Bard, *J. Phys. Chem. B*, 1999, **103**, 10469–10480.
10 F. Kanoufi, Y. Zu and A. J. Bard, *J. Phys. Chem. B*, 2001, **105**, 210–216.

11 K.-F. Chow, B.-Y. Chang, B. A. Zaccheo, F. Mavré and R. M. Crooks, *J. Am. Chem. Soc.*, 2010, **132**, 9228–9229.
12 K.-F. Chow, F. Mavré, J. A. Crooks, B.-Y. Chang and R. M. Crooks, *J. Am. Chem. Soc.*, 2009, **131**, 8364–8365.
13 W. Zhan, J. Alvarez and R. M. Crooks, *Anal. Chem.*, 2003, **75**, 313–318.
14 W. Zhan, J. Alvarez, L. Sun and R. M. Crooks, *Anal. Chem.*, 2003, **75**, 1233–1238.
15 R. K. Anand, E. Sheridan, K. N. Knust and R. M. Crooks, *Anal. Chem.*, 2011, **83**, 2351–2358.
16 W. Zhan and R. M. Crooks, *J. Am. Chem. Soc.*, 2003, **125**, 9934–9935.
17 J. P. Guerrette, S. M. Oja and B. Zhang, *Anal. Chem.*, 2012, **84**, 1609–1616.
18 J.-Y. Park, B.-Y. Chang, H. Nam and S.-M. Park, *Anal. Chem.*, 2008, **80**, 8035–8044.
19 F. Frantzen, K. Grimsrud, D. E. Heggli, A. L. Faaren, T. Lovli and E. Sundrehagen, *Clin. Chem.*, 1997, **43**, 2390–2396.
20 B.-Y. Chang, J. A. Crooks, K.-F. Chow, F. Mavré and R. M. Crooks, *J. Am. Chem. Soc.*, 2010, **132**, 15404–15409.
21 Y. Xia and G. M. Whitesides, *Angew. Chem., Int. Ed.*, 1998, **37**, 550–575.
22 F. Mavré, K.-F. Chow, E. Sheridan, B.-Y. Chang, J. A. Crooks and R. M. Crooks, *Anal. Chem.*, 2009, **81**, 6218–6225.
23 B.-Y. Chang, F. Mavré, K.-F. Chow, J. A. Crooks and R. M. Crooks, *Anal. Chem.*, 2010, **82**, 5317–5322.
24 B.-Y. Chang and S.-M. Park, *Annu. Rev. Anal. Chem.*, 2010, **3**, 207–229.
25 A. J. Bard and L. R. Faulkner, *Electrochemical Methods: Fundamentals and Applications*, John Wiley & Sons, Inc., New York, 2nd edn, 2001.
26 W. Hyk and Z. Stojek, *Anal. Chem.*, 2002, **74**, 4805–4813.
27 W. J. Miao, J. P. Choi and A. J. Bard, *J. Am. Chem. Soc.*, 2002, **124**, 14478–14485.
28 G. Y. Shi, Z. Y. Sun, M. C. Liu, L. Zhang, Y. Liu, Y. H. Qu and L. T. Jin, *Anal. Chem.*, 2007, **79**, 3581–3588.
29 S. E. Fosdick and R. M. Crooks, *J. Am. Chem. Soc.*, 2012, **134**, 863–866.